ARTICLE

OBC
www.rsc.org/obc

The effects of substrate orientation on the mechanism of a phosphotriesterase†

Colin J. Jackson, Jian-Wei Liu, Michelle L. Coote* and David L. Ollis*
Research School of Chemistry, Australian National University, Canberra, ACT 0200, Australia. E-mail: ollis@rsc.anu.edu.au,, mcoote@rsc.anu.edu.au; Fax: +61 2 6125 0750

Received 6th September 2005, Accepted 6th October 2005
First published as an Advance Article on the web 16th November 2005

While the underlying chemistry of enzyme-catalyzed reactions may be almost identical, the actual turnover rates of different substrates can vary significantly. This is seen in the turnover rates for the catalyzed hydrolysis of organophosphates by the bacterial phosphotriesterase OpdA. We investigate the variation in turnover rates by examining the hydrolysis of three classes of substrates: phosphotriesters, phosphothionates, and phosphorothiolates. Theoretical calculations were used to analyze the reactivity of these substrates and the energy barriers to their hydrolysis. This information was then compared to information derived from enzyme kinetics and crystallographic studies, providing new insights into the mechanism of this enzyme. We demonstrate that the enzyme catalyzes the hydrolysis of organophosphates through steric constraint of the reactants, and that the equilibrium between productively and unproductively bound substrates makes a significant contribution to the turnover rate of highly reactive substrates. These results highlight the importance of correct orientation of reactants within the active sites of enzymes to enable efficient catalysis.

Introduction

The toxic effect of organophosphorus triesters, most importantly their inhibition of acetylcholinesterase (AChE), has resulted in their widespread use in agriculture as pesticides and their synthesis as chemical warfare agents. Occupational or intentional exposure to organophosphates is a continuing health hazard,[1] which has led to the detailed study of enzymes capable of catalyzing their hydrolysis and detoxification.[2] The chemical structures of three organophosphate pesticides are shown in Table 1: the phosphorothiolate dimethoate (DMO), and the phosphothionates methyl parathion (MPS) and methyl chlorpyrifos (MCS), in addition to their oxono-substituted analogues methyl paraoxon (MPO) and methyl chlorpyrifos oxon (MCO). Phosphotriesterases capable of degrading these compounds have been isolated from soil bacteria found in contaminated areas. These include the closely related phosphotriesterases from *Pseudomonas diminuta* MG (PTE)[3] and *Agrobacterium radiobacter* (OpdA).[4] The potential use of these enzymes for the detoxification of organophosphate pesticides and related chemical warfare agents such as VX and sarin, has increased interest in understanding the catalytic mechanism and improving their activity.

OpdA[4] is very similar to PTE[3] in sequence and structure, and it is assumed that their mechanisms are essentially identical.[5] The structures of OpdA and PTE have been solved crystallographically and both adopt an $(\alpha/\beta)_8$ barrel tertiary structure. The active site contains a carboxylated lysine coordinating a binuclear metal centre, bridged by an hydroxide. The α-metal (as defined by Benning *et al.*[6]) is coordinated by the residues His55, His57, and Asp301, and the β-metal by His201 and His230.[5,6] The catalytic mechanism is relatively well understood and is proposed to involve coordination of the P=O/S group of the substrate by the β-metal, followed by attack from a hydroxide nucleophile, deprotonated by the α-metal, at the electrophilic phosphorus centre, and departure of the leaving group in an S_N2-type, or addition–elimination, reaction.[7,8] This mechanism allows these enzymes to degrade a broad range of phosphotriester substrates at varying rates; for instance, PTE catalyzes the hydrolysis of parathion extremely efficiently ($k_{cat}/K_m = 2 \times 10^7$ s^{-1} M^{-1}),[9] while the efficiency of chlorpyrifos hydrolysis is considerably lower ($k_{cat}/K_m = 2.8 \times 10^5$ s^{-1} M^{-1}).[10]

There has been considerable theoretical work on the subject of phosphotriester hydrolysis, largely concentrated on trimethyl phosphate (TMP) and its close analogues,[11–13] although the hydrolysis of ethyl paraoxon and related phosphofluoridate nerve agents have also been investigated.[14] This latter study, by Zheng *et al.*, demonstrated that the gas-phase hydrolysis of paraoxon occurred in a single step, and is consistent with experimental work demonstrating that PTE catalyzed hydrolysis occurs by an S_N2-type, or addition–elimination, reaction with net inversion of

Table 1 The structures of the organophosphates discussed in this work, using the general structure $Z{=}P(OCH_3)_2R$

Z	R	Abbreviation	Full name
S	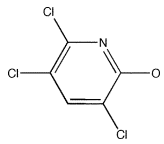	MCS	Methyl Chlorpyrifos Thion
O	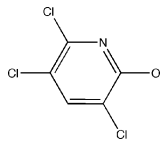	MCO	Methyl Chlorpyrifos Oxon
S	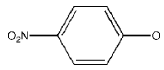	MPS	Methyl Parathion
O	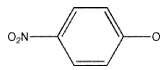	MPO	Methyl Paraoxon
S	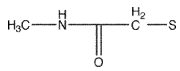	DMO	Dimethoate
O		TMP	Trimethyl Phosphate

† Electronic supplementary information (ESI) available: Potential energy surface surrounding the MCO hydrolysis transition state. Geometries of reactants, intermediates, transition states and products. The relative energy change as a function of the distance between Co^{2+} and MPS or OH^-. GAUSSIAN archive entries. See DOI: 10.1039/b512399b

DOI:10.1039/b512399b

stereochemistry at the phosphorus centre.[15] The work of Zheng *et al.*, also indicated that calculations of paraoxon hydrolysis in the gas-phase were more consistent with the kinetic data for the PTE-catalyzed hydrolysis than calculations incorporating solvent effects. This is not unexpected, as the hydrophobic active sites of PTE and OpdA exclude almost all solvent molecules other than those involved in the reaction (the water/hydroxide nucleophile), or in hydrogen bond networks within the protein.[7] Although the calculations confirmed the nature of the reaction, further comparison between the theoretical calculations and the PTE-catalyzed hydrolysis was made in the belief that the nucleophile in the reaction was the hydroxide bridging the two metals. More recent experiments suggest that the nucleophile is more likely to be a terminally bound and deprotonated water molecule that is ~1 Å closer to the phosphorus of the bound substrate.[7] Accordingly, an accurate explanation of how the phosphotriesterases lower the activation energy of the reaction has not yet been achieved.

In contrast to the hydrolysis of paraoxon, the nature of the hydrolysis of the phosphothionate substrates has not been studied theoretically. Experimentally, it has been shown that they are hydrolyzed less rapidly by PTE with zinc ions in the active site, and that the catalytic rate is increased if the zinc ions are replaced by cobalt.[16] It has been assumed that this is a result of increased polarization of the P=S bond, however this has not been established. In addition, there exist significant differences in the turnover rates of highly similar phosphotriester and phosphothionate substrates; for instance, ethyl chlorpyrifos (thion) is hydrolyzed at approximately one thousandth the rate of ethyl paraoxon.[3] This is interesting because the data are inconsistent with the current understanding of the mechanism, and chlorpyrifos, widely used since 1965, is resistant to enhanced biodegradation in soil.[17] Characterization of P–S bond hydrolysis in phosphorothiolates has also been less thorough than that of P–O bond hydrolysis. Theoretical calculations have demonstrated that a stable pentacoordinate intermediate is formed during P–S bond peroxidolysis of an analogue of VX in aqueous solution.[18] Whether this also occurs during the hydrolysis of phosphorothiolate pesticides, which differ in that they do not possess any phosphonate bonds, is still unknown.

In the present work we address three unresolved questions relating to the mechanism of the bacterial phosphotrieserases through a comparative experimental–theoretical approach. (i) How does OpdA lower the activation energy, and catalyze the hydrolysis of these substrates? (ii) Is there a mechanistic explanation for the experimentally observed differences in the turnover of phosphotriesters and phosphorothiolates? (iii) Is the difference in turnover rate between phosphotriesters and their phosphothionate analogues a result of differential polarization by active site metals, or a consequence of non-productive binding? To answer these questions we have adopted a comparative theoretical–experimental approach. High level *ab initio* calculations of the gas-phase hydrolysis reactions are used to determine the intrinsic reactivities of the various substrates and analyze their reaction pathways. These are then compared with the experimentally determined kinetic constants and structural data. It should be emphasized that the aim of the study is not to establish that these calculations are a realistic model for the enzyme-catalyzed hydrolysis; rather, by examining the differences between the theoretical data and experimental results, we can describe the role the enzyme plays in catalysis.

Results and discussion

To address the unanswered questions relating to the mechanism of the bacterial phosphotriesterase OpdA, we have conducted a thorough investigation into the nature of the hydrolysis of a broad range of substrates, including the phosphotriesters MPO, MCO and TMP, the phosphothionates MPS and MCS and the phosphorothiolate DMO. Experimentally determined kinetic constants are shown in Table 2. These demonstrate that, while MPS, MPO and MCO are all hydrolyzed rapidly, MCS and DMO are hydrolyzed at considerably lower rates and TMP is not hydrolyzed at detectable levels. To complement these results, we have also calculated the stationary points on the minimum energy paths for each reaction (see Table 2 and Fig. 1). Based on the theoretical results, all reactions, with the exception of TMP, are highly exothermic and there are no major differences in the magnitude of the barriers for the formation of transition states. It is also clear that while MPS, MPO, MCS and MCO are hydrolyzed *via* effectively identical one-step reactions, DMO and TMP pass through several intermediates. Comparison between the experimentally determined kinetic constants and the calculated potential energy surfaces highlights inconsistencies in our understanding of the mechanism. For instance, the turnover of DMO is significantly slower than that of MPS, the hydrolysis of TMP is not significantly catalyzed, the process by which OpdA lowers the activation energy to catalyze the reaction is unknown, and there is a several hundred fold difference in the turnover rate of similarly highly reactive substrates such as MCS and MPS. To address these issues we examined the chemical basis for the rapid hydrolysis of a model substrate, parathion, and compared this to the hydrolysis of DMO and TMP, examining the causes of the large reductions

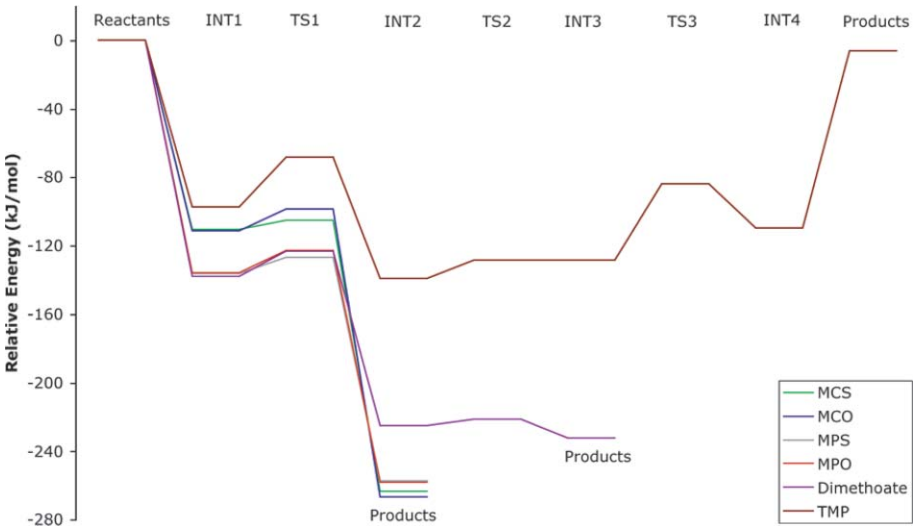

Fig. 1 Relative free energies (0 K, kJ mol^{-1}) for the gas-phase reaction of OH^- with MCS, MCO, MPS and MPO as calculated at the RMP2/6-311 + G(3df,2p)//B3-LYP/6-31 + G(d) level of theory. The zero of energy corresponds to the reactants at infinite separation.

Table 2 Change in free energy (0 K, kJ mol^{-1})[a] for the hydrolysis of MCS, MCO, MPS, MPO, DMO and TMP. Experimentally determined kinetic constants are shown below[b]

	MCS	MCO	MPS[c]	MPO	DMO	TMP
Reactants	0.0	0.0	0.0	0.0	0.0	0.0
INT1	−110.5	−111.4	−136.2	−136.1	−137.9	−97.3
TS1	−105.2	−98.8	−127.0	−122.6	−123.3	−68.3
INT2/Products	−263.3	−266.6	−257.3	−258.2	−225.1	−139.3
TS2	—	—	—	—	−221.4	−128.7
INT3/Products	—	—	—	—	−232.3	−128.7
TS3	—	—	—	—	—	−83.9
INT4	—	—	—	—	—	−109.6
Products	—	—	—	—	—	−6.2
k_{cat}/s^{-1}	1.6	1900	1200	2500	4.2	N/D[d]
K_m/μM	85	150	100	230	480	N/D[d]
(k_{cat}/K_m)/s^{-1} M^{-1}	1.8×10^4	1.3×10^7	1.2×10^7	1.1×10^7	9×10^3	N/D[d]

[a] Calculated at the RMP2/6-311 + G(3df,2p) using B3-LYP/6-31 + G(d) geometries and scaled B3-LYP/6-31 + G(d) zero-point vibrational energy. [b] Error is below 10% for the calculation of kinetic constants of dimethoate and MCO, and below 15% for MCS. [c] Experimentally determined kinetic constants for the hydrolysis of MPS and MPO by OpdA have been taken from a previous study by Yang *et al.* (2003).[5] [d] Not detectable (below the limit of detection).

in the turnover number of the latter substrates. Furthermore, we discuss the probable cause of the slow hydrolysis of MCS, relative to the close analogues MPS, MPO and MCO.

Mechanistic differences in the hydrolysis of fast and slow substrates

OpdA was isolated from soil contaminated with the organophosphate pesticide parathion[4] and it is reasonable to assume that this is the 'natural' substrate of the enzyme in the sense that this is the substrate which OpdA has evolved to degrade. This is also consistent with kinetic results demonstrating that both OpdA and PTE hydrolyze parathion and MPS at rates approaching the diffusion limit.[5,8] Dimethoate (DMO) and other phosphorothiolate pesticides are known to be hydrolyzed at significantly lower rates than parathion and to inhibit the hydrolysis of phosphotriesters uncompetitively.[5,19] Results from enzyme kinetics demonstrate that DMO is hydrolyzed at comparable rates to other phosphorothiolates, such as demeton[5] (Table 2). Trimethyl phosphate (TMP) is not detectably hydrolyzed by OpdA (Table 2), and results from crystal soaking experiments demonstrate that it binds unproductively in the active site of OpdA.[7] Results from enzyme kinetics are suggestive of significant mechanistic differences in the hydrolysis of 'fast' substrates such as MPS and 'slow' substrates such as DMO.[8,16] These studies demonstrated, through the use of Brønsted plots, that there is no chemical barrier for the hydrolysis of 'fast' substrates such as MPS, and that their hydrolysis is diffusion limited. In contrast, the large negative β_{lg} values observed for the hydrolysis of 'slow' substrates strongly indicated that during the hydrolysis of these substrates bond cleavage is rate limiting, and predict that the transition state is significantly dissociative and product-like.

We calculated the geometries of the reaction coordinates, and their respective energies, for MPS, DMO and TMP. These results demonstrate that in the case of MPS, the reaction proceeds through a hydrogen bonded intermediate and one transition state in an S_N2-type mechanism (Table 2, Figs. 1, 2). This is predicted to be an extremely rapid reaction, and is consistent with the biochemical results[15] and previous theoretical work on the hydrolysis of paraoxon.[14] The only energy barrier to this reaction is that between the intermediate and transition state (9.2 kJ mol^{-1}). In the case of DMO, calculations show that after reaching the first transition state, the course of DMO hydrolysis differs from that of MPS (Table 2, Figs. 1, 2): the

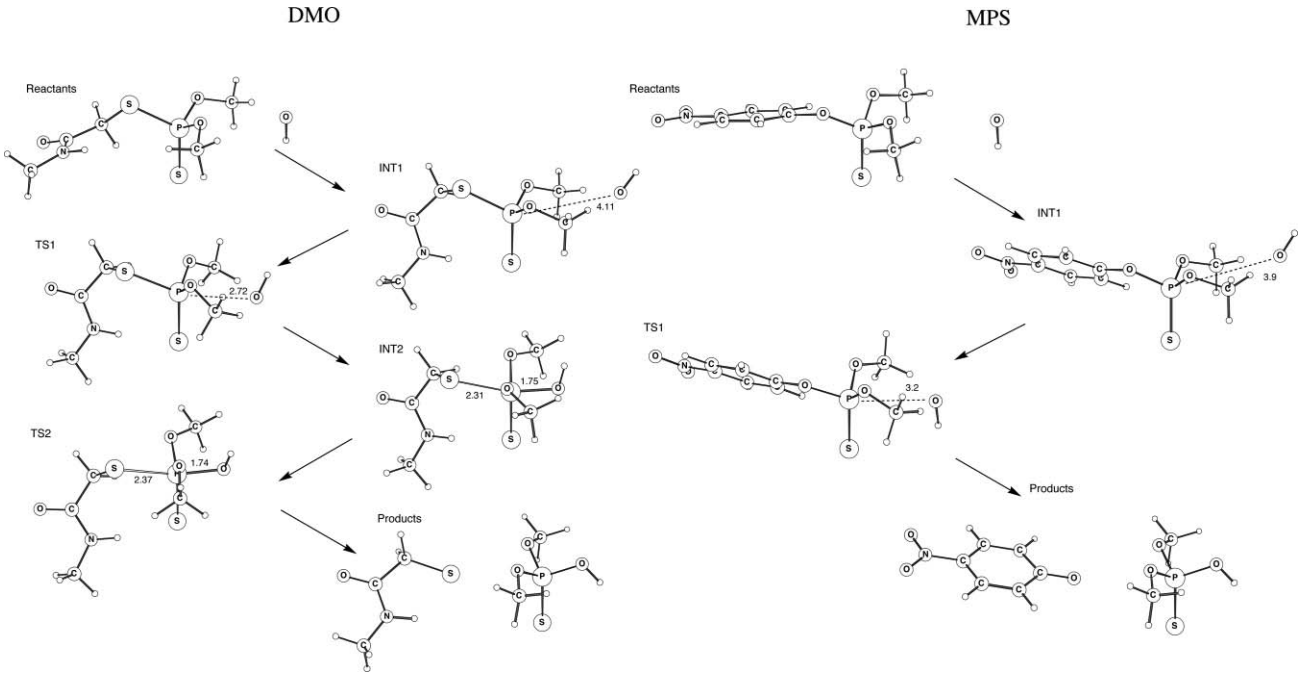

Fig. 2 B3-LYP/6-31 + G(d) geometries of the reactants, intermediates, transition states and products formed during the gas-phase reaction of OH$^-$ with MPS and DMO.

attack of the hydroxide nucleophile at the electrophilic centre of dimethoate leads to the formation of a pentacoordinate intermediate, which then decomposes to form the products. The energy barrier for the formation of the first transition state is 14.6 kJ mol^{-1}, comparable to the 9.2 kJ mol^{-1} barrier in the equivalent step in parathion hydrolysis, and 4.4 kJ mol^{-1} for the formation of the second transition state. Calculated reaction coordinates and energies for the hydrolysis of TMP (Table 2, Fig. 1, ESI Fig. 3†), were consistent with previous studies at lower levels of theory[11–13] and show a significant difference in the potential energy landscape, compared to those of MPS or DMO, in that after the formation of the pentacoordinate intermediate significant energy is required to remove the leaving methoxide group. The energy barriers to the first and second transition states (27.5 and 11.8 kJ mol^{-1}) are also higher than the comparable barriers in dimethoate hydrolysis, consistent with the poor leaving group.

Comparison between these results for the gas-phase hydrolysis and the results of enzyme kinetics and crystallographic experiments, allows us to determine at which point during the hydrolysis the phosphotriesterases lower the activation energy of the reaction, achieving catalysis. It is known that there is no chemical barrier to the hydrolysis of 'fast' substrates such as MPS, and that the hydrolysis of 'slow' substrates such as DMO is limited by bond cleavage, and the energy barrier to a product-like transition state.[16] This is consistent with OpdA catalyzing these reactions through lowering the activation energy required to achieve the first transition state, but not the second 'product-like' transition seen in the hydrolysis of DMO (Table 2, Figs. 1, 2). In addition, crystallographic studies, in which crystals of OpdA were soaked in solutions of various substrates, produced an enzyme–product complex through DMO soaking; in contrast, no bound product was observed after MPS soaking.[7] This is consistent with the formation of a pentacoordinate intermediate in the case of DMO hydrolysis, bound dually to the two metals, which decomposes and leaves dimethyl phosphate bound at the active site. In the case of MPS hydrolysis, we propose that no pentacoordinate intermediate forms, allowing rapid departure of the product, consistent with the diffusion limited kinetics (Table 2). A mechanistic scheme is shown in Fig. 3. This also explains several inconsistencies in the turnover of phosphotriesters and phosphorothiolates, such as the uncompetitive inhibition of phosphotriester hydrolysis by phosphorothiolates:[19] once DMO is hydrolyzed, enzymes with dimethyl thiophosphate bound in the active site cannot participate in the reaction until the product is displaced. This will cause a reduction in the V_{max} of the enzyme for the hydrolysis of rapidly hydrolyzed phosphotriesters such as MPS, but little effect on the K_m as the affinity of the remaining enzymes for parathion will be unchanged. These calculations have therefore clarified the conclusions drawn from previous crystallographic and kinetic work and enabled an extremely detailed understanding of the mechanism.

The mechanism of catalysis

With this strong evidence that OpdA lowers the energy barrier to the first transition state in substrate hydrolysis, it is worth investigating the means by which this catalysis is achieved. Recent crystallographic work established the binding mode of substrates in OpdA.[7] When the optimized geometry of MPS is modelled into the active site (in the only reasonable orientation possible), it requires tilting of the P-centre toward the nucleophile to be accommodated. The P–OH$^-$ distance observed in this modelling is 3.1 Å. When compared to the gas-phase calculations, it is clear that the active site surface therefore accomplishes a significant reduction in the activation energy required for the reaction, shortening the distance between the electrophilic phosphorus and nucleophilic hydroxide beyond

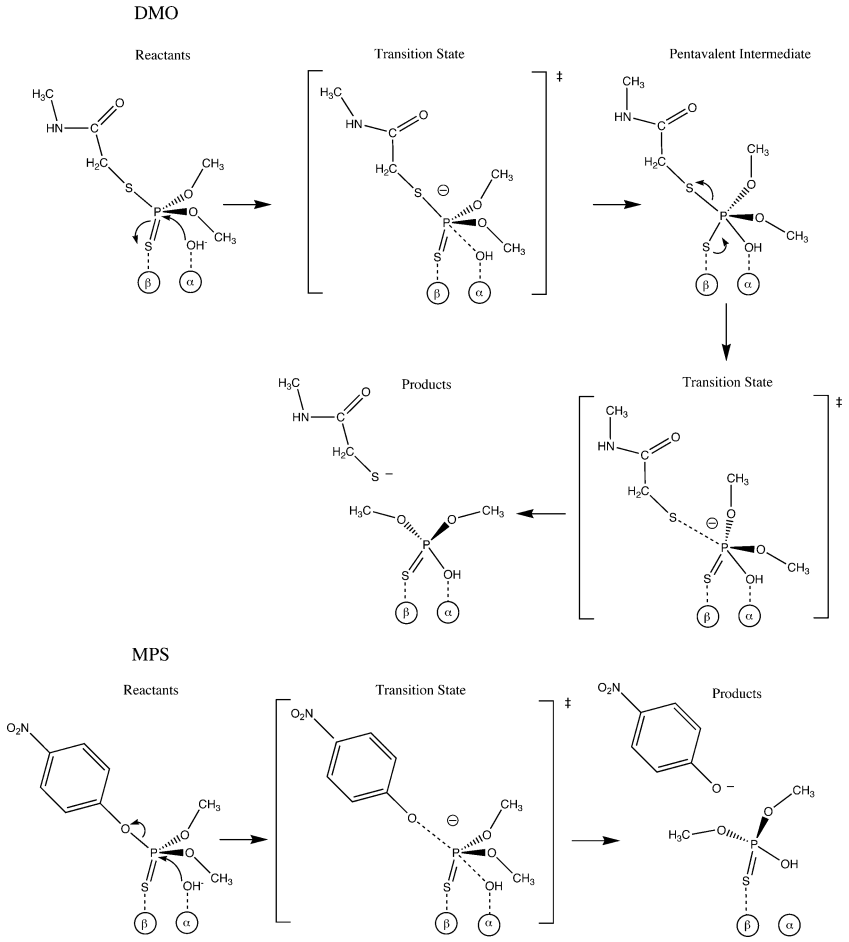

Fig. 3 A mechanistic scheme for the hydrolysis of DMO and MPS by OpdA.

the intermediate (3.9 Å), approaching that of the transition state (3.2 Å) (Figs. 1, 2). This proposal is further supported when compared to the binding of the, uncatalyzed, potential substrate TMP. The potential energy surface demonstrates that the formation of an intermediate should be possible and is not significantly different to the formation of an intermediate during DMO hydrolysis (Table 2, Fig. 1). However, the crystal structure of an OpdA–TMP complex, with a water/hydroxide bound at the β-metal and a TMP molecule bound at the α-metal, showed no indication of any significant interaction between the nucleophile and the electrophilic phosphorus of TMP.[7] The binding of TMP is therefore non-productive because the substrate is small enough for no tilting to occur (unlike larger substrates such as MPS), and no contribution is made to the activation energy. This results in the reaction remaining in the bottom of the first 'well' (Fig. 1), with the nucleophile 3.8 Å away from the electrophilic phosphorus. The comparison between the theoretical and experimental results from this study (Table 2) and previous structural work[7] has allowed the proposal of a reasonable explanation for the mechanism by which OpdA lowers the activation energy (through steric constraint of the reactants) to the fist transition state, and highlights the often overlooked importance of nucleophile–electrophile distances in enzyme mechanisms.

The 'slow' turnover of the phosphothionate MCS

There is currently no reasonable explanation for the slow turnover of ethyl chlorpyrifos (ECS), or MCS in the literature. Kinetic analysis demonstrates that MCS is hydrolyzed approximately 10^3 times slower than MCO and other diffusion-limited substrates such as MPO and MPS (Table 2), consistent with previous kinetic data regarding the turnover of ECS by PTE.[3] To examine the process of MCS hydrolysis, the geometries of the reaction coordinates were calculated, as were their respective energies. As seen in Fig. 1 (ESI Fig. 2†) and Table 2, the gas-phase hydrolysis of MCS is essentially identical to that of the other three substrates. It is a one-step single in line displacement mechanism, and the energy barrier for the formation of the transition state is actually less than for the MPS transition state (5.3 kJ mol^{-1}, compared to 9.2 kJ mol^{-1}). Therefore, there appears to be no chemical basis for the extremely slow turnover of MCS and the rate must be inhibited by some other factor.

Importantly, the similarity between the 4 substrates analyzed here demonstrates that the increased polarity of the P=O bond in the oxono analogues does not make a significant contribution to the rate of hydrolysis, which is consistent with the highly exothermic nature of the reaction. Additionally, previous investigations of PTE involving enzyme kinetics has demonstrated that for both paraoxon and parathion, the rate limiting step is unrelated to the cleavage of the P–O bond.[8] Therefore, in this case, increasing the polarization of the P=O or P=S bond through the use of different metals in the active site would not affect the rate. It should also be noted that the rapid hydrolysis of MCO (Table 2) suggests that the leaving group of MCS is not directly responsible for the slow turnover.

Non-productive binding

One possible cause of the slow turnover of MCS is non-productive binding. Non-productive binding is seldom considered in enzyme kinetics, largely because it is difficult to quantify. It has been characterized previously in chymotrypsin[20,21] and glutathione transferase,[22] and the concept is straightforward. If a substrate binds in the active site of an enzyme in an orientation that will not allow hydrolysis, the K_m will not be significantly affected since the affinity for the substrate remains the same, but the k_{cat} will be reduced as the number of enzyme molecules available to catalyze the hydrolysis will be reduced. The enzyme will not be able to catalyze hydrolysis until the substrate either diffuses out, or reorients. In effect, it is a form of substrate inhibition, but one that is not readily measurable. We observe this relationship in the hydrolysis of MCO and MCS (Table 2): both have comparable values of K_m, while k_{cat} varies by a factor of approximately 10^3, without any clear chemical basis. Accordingly, the catalytic mechanism for the hydrolysis of phosphotriesters and phosphothionates may be more accurately described as follows:

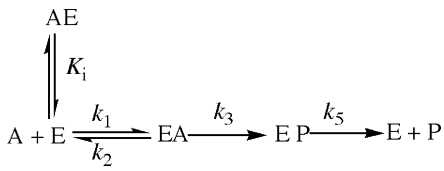

(1)

In this scheme (eqn. 1), the inhibition caused by non-productive substrate binding is indicated by K_i (modified from refs. 8,21).

Although the example of TMP does establish that non-productive binding can occur in OpdA,[7] the mode of binding is unlikely to be related to MCS, as MCS is too large to bind at the α-metal. Another crystallographic example of non-productive binding, this time in PTE, was therefore investigated.[23] Co-crystallization experiments with substrate analogues of methyl paraoxon in which the P–O bond was replaced by a non-hydrolysable phosphono P–C bond produced a PTE–diethylbenzyl phosphonate (DEBP) complex. This structure is interesting because the analogue is bound at the active site in an unexpected mode, with the leaving group in a side chain pocket, a side chain in the leaving group channel and no significant electronic interaction between the β-metal and the P=O group. When the analogue is modelled into the active site in the same manner as MPS, it clearly clashes with the amino acids of the leaving group channel because of the different orientation of the aromatic compared to methyl parathion (Fig. 4). The cause of the non-productive binding therefore

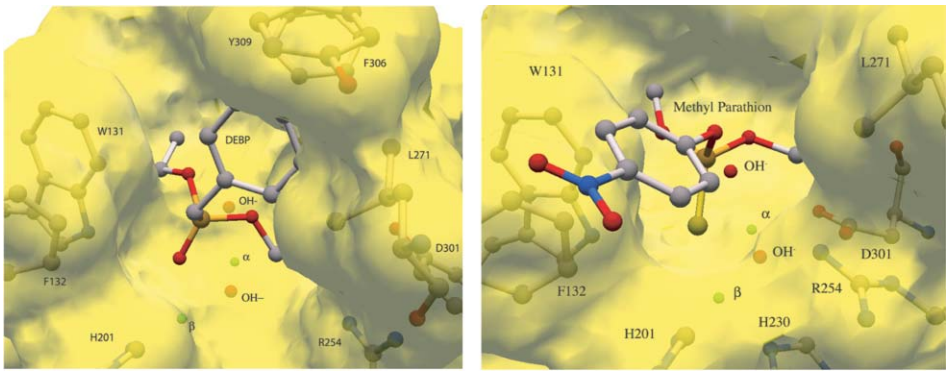

Fig. 4 MPS and DEBP modelled into the active site of OpdA. The molecular surface is shown to highlight the interaction of the molecules with the enzyme. The diagram of MPS modelled into the active site was taken from Jackson *et al.*, 2005.[7]

Table 3 Relative free energies (0 K, kJ mol^{-1})[a] for different conformers of MCS, MCO, MPS, MPO and DEBP, and the transition states between them

Ring orientation	MCS	MCO	MPS	MPO	DEBP
Sideways	0.0	0.0	0.0	0.0	0.0
TS	23.5	21.3	11.6	12.6	12.3
Upwards	8.5	7.3	4.1	5.0	−2.7

[a] Calculated at the RMP2/6-311 + G(3df,2p) using B3-LYP/6-31 + G(d) geometries and scaled B3-LYP/6-31 + G(d) zero-point vibrational energy.

lies in the steric interactions between DEBP and the enzyme which force the analogue to bind in the only conformation possible. Substrate binding in OpdA will depend upon three major factors: (i) steric interactions between the substrate and the enzyme, (ii) electronic interactions between the β-metal and the substrate, and (iii) hydrophobic interactions between the substrate and the hydrophobic pockets of the active site.

The structure of DEBP bound in the active site of PTE was of further interest because of the large conformational differences between itself and the substrates it was supposed to mimic, such as MPS and MPO. As seen in Fig. 4, the angle of the P–C–C phosphono bond to the leaving group in DEBP is markedly different to that of the analogous P–O–C bond in MPS. We determined whether this conformation was the lowest energy structure, or whether its conformation had been altered by PTE. At the B3-LYP 6-31 + G(d) level of theory, the lowest energy structure is that with the ring pointed outward in the same manner as the leaving group of MPS; however, the higher level RMP2/6-311 + G(3df,2p) calculations show that the structure observed in PTE is in fact the lowest energy conformer (Table 3). Table 3 and ESI Fig. 4† demonstrate that the lowest energy geometries of MPS, MPO, MCS and MCO are all essentially identical (MPO has its ring rotated 90 degrees, but as it is turned over at approximately the same rate as MPS and MCO it clearly plays no significant role). Accordingly, we investigated whether the equilibrium between conformations of MCS favoured a conformation that could bind non-productively with greater affinity. To do this, we optimized the geometries and calculated the energies, of all four substrates with the ring pointed upwards as it is in the lowest energy conformer of DEBP. In addition, we calculated the rotational barriers for the transition states separating the two conformations (ESI Fig. 4†, Table 3). These demonstrate that the energy barrier for conversion between the two conformers is in fact lowest for MPO and MPS, and that there is no significant difference between the conformation of MCS and the other three substrates, excluding steric interactions as the cause of non-productive binding.

Another possible cause of non-productive binding is the hydrophobicity of the substrates. The chemical differences between oxono and thiono analogues of organophosphorus compounds have been studied in detail by Maxwell and Brecht.[24] They demonstrated that the P=S moiety makes the substrates considerably more hydrophobic than those with the P=O group, as a result of the reduced polarization of the P=O/S bond. This was proposed to cause non-productive binding of these groups in acetylcholinesterase (AChE), and contribute to the significant reduction in inhibition of AChE by thiono analogs (1240 fold for parathion/paraoxon). The relative V_{max} of PTE for 5 highly reactive ethyl-substituted phosphotriester substrates (paraoxon > parathion ≥ coumaphos > diazinon > chlorpyrifos) is more consistent with their hydrophobicities (2.31, 3.84, 3.87, 3.42, 4.77, in Log*P*) than the pK_a of the leaving group (7.25, 7.25, 8.97, 1.17, 7.5).[3] Similarly, the relative k_{cat} of OpdA for the 4 highly reactive methyl-substituted phosphotriester substrates discussed in this study (MPO 2500 s^{-1}, MCO 1900 s^{-1}, MPS 1200 s^{-1}, MCS 1.6 s^{-1}) shows the same trend toward the relative hydrophobicity (1.5, 2.7, 2.9, 3.7, in Log*P*).

If a substrate the size of MCS becomes coordinated to the β-metal, *via* the P=O/S group, it will be oriented correctly for hydrolysis; there is no other mode of binding at the metal possible. However, as the PTE–DEBP complex demonstrates, it is possible for molecules to bind at the active site without significant interaction with the metal.[23] Another result consistent with this proposal was found in a molecular dynamics study of substrates within the active site of PTE, and demonstrated that paraoxon could bind in a non-productive orientation in addition to the correct orientation.[25] As we have shown, MCS and MPO are structurally very similar, so it would be expected that this result would extend to MCS. This may then provide the best explanation for the non-productive binding of MCS.

It has been established that thiono compounds, such as MPS and MCS, are turned over at significantly faster rates by OpdA and PTE in which the Zn^{2+} active site metals are replaced by Co^{2+}.[16] This has previously been assumed to result from increased polarization of the P=S bond by cobalt, owing to its greater affinity for sulfur than the affinity of zinc for sulfur, according to the hard–soft acid–base theory. However, as we have shown, the reaction is sufficiently exothermic for the small difference in the polarization of this bond by different metals, and the associated change in the electrophilicity of the phosphorus between oxono and thiono analogues, not to contribute to the reactivity (Table 2, Fig. 1). The strength of the interaction between the sulfur of MPS and Co^{2+} in the active site environment of OpdA was analyzed theoretically, and results suggest it is insufficient to allow formation of a stable Co^{2+}–MPS complex, in contrast to the formation of a stable complex with a hydroxide (ESI Fig. 5†), which is not surprising considering the neutral character of MPS. This also supports the notion that the contribution of increased polarization will be small relative to the reactivity of the substrates, and that hydrophobic interactions between MPS and the active site cavity play an equally important role in substrate binding. The increased turnover rate of phosphothionate substrates in Co^{2+}-substituted enzymes is therefore more likely to be a consequence of the greater affinity of cobalt for sulfur, which shifts the binding equilibrium of the substrates away from non-productive binding based solely on hydrophobic interactions, toward productive binding as a result of hydrophobic and metal interactions, consequently resulting in more hydrolysis. It should be noted that the most hydrophobic substrates will have the least polar distribution of charge; accordingly, the correlation between activity and hydrophobicity is likely to result from both the affinity of hydrophobic groups with hydrophobic pockets, and the attraction between the charge on the coordinating P=O/S group and the β-metal.

This explanation is consistent with the work of other groups: Cho *et al.*,[10] identified mutations in PTE, remote from the active site (A80V, K185R, I274N), that increased the global hydrolysis rate for a range of organophosphate pesticides (paraoxon, parathion, coumaphos, chlorpyrifos). These mutations typically increased the k_{cat} in the order of 10 to 50 fold for paraoxon, parathion and coumaphos, while the increase in the k_{cat} toward chlorpyrifos was ~500 fold. It has been suggested that the A80V and K185R mutations achieve this enhancement in activity by stabilizing PTE in a more active conformation.[5,10] If this conformation were more active because it enhanced substrate orientation and correct binding, the biggest difference would be seen in the catalysis of the substrate with the highest probability to bind incorrectly, *i.e.*, chlorpyrifos or MCS. That work further complements this study by demonstrating that PTE containing Co^{2+} hydrolyses chlorpyrifos at significantly higher rates than PTE containing Zn^{2+},[3] and that an essentially identical active site is capable of catalyzing hydrolysis of MCS at rates close to the diffusion limit, highlighting the extremely labile nature of the substrate. Therefore, although several factors are likely to influence the turnover rate of highly reactive substrates such as MPS and MCS, the hydrophobicity of the substrates and the

associated probability that they will bind in an orientation in which hydrolysis can occur, makes a significant contribution.

Experimental

Materials

All chemicals were purchased from Sigma-Aldrich unless otherwise noted. Methyl chlorpyrifos oxon (MCO), methyl chlorpyrifos thion (MCS) and dimethoate were purchased from Chem Service (PA, USA). Bacto-tryptone and Bacto-yeast extract were purchased from Difco laboratories. The purity of the organophosphates was >95% as stated by the manufacturers. Molecular biology reagents were purchased from New England Biolabs or Roche Molecular Diagnostics (Australia) unless otherwise stated. Pfu DNA polymerase was purchased from Stratagene (CA, USA). The Overnight Express™ autoinduction system was purchased from Novagen (WI, USA).

Bacterial strains and plasmids

The plasmid used to purify OpdA (NCBI protein sequence database accession number: AAK85308) was constructed by cloning OpdA between NcoI and BamHI sites in pTrcHisB (Invitrogen). The primers used to amplify the gene were: fp 5′ TTAAATAAGGAGGAATAAACCATGG 3′ and rp 5′ TCTCGAGCTCGGATCCCGTTATTAC 3′. The plasmid was expressed in *E. coli* DH5α cells (Invitrogen) grown in Luria–Bertoni (LB) medium. Growth media were supplemented with ampicillin (100 mg L^{-1}). GpdQ was expressed from the pCY76 vector as described previously.[26]

Preparation of purified phosphotriesterase

Wild-type OpdA was produced and purified as follows: the plasmid was expressed using the Overnight Express™ autoinduction system (Novagen) at 37 °C. Cells were harvested by centrifugation, then resuspended and lysed in 10 mL of 20 mM Tris.Cl pH 8.0, containing BugBuster™ protein extraction reagent (Novagen) and 1 mg mL^{-1} of chicken egg lysozyme (incubated at room temperature for 30 min). The insoluble matter was pelleted and the soluble fraction was twice passed through a regenerated 1 mL pre-packed DEAE–Fractogel column (Amersham Biosciences) that had been pre-equilibrated with 20 mM Tris.Cl pH 8.0. Powdered ammonium sulfate was added to the active flow-through fractions to a final concentration of 0.5 M and stirred for 10 min at 4 °C. The solution was centrifuged at 30 000 g for 30 min. The active soluble fraction was loaded onto a 1 ml pre-packed phenyl-sepharose HP column (Amersham Biosciences). A linear ammonium sulfate gradient (0.5–0 M) was applied over 10 column volumes to elute the bound protein. Eluted fractions were assayed for phosphotriesterase activity by assaying 1 μL of eluate in 100 μL of 10 μM coumaphos-o-analogue, 100 mM Tris.Cl pH 8.0 and by observing fluorescence under UV light. Phosphotriesterase activity eluted at ~0.35 M ammonium sulfate. SDS-PAGE analysis of pooled active fractions indicated that the purified OpdA was essentially homogeneous. The purified protein was dialyzed against 20 mM HEPES, 150 mM NaCl, pH 7.5, 100 μM $ZnCl_2$ overnight before being assayed. Protein concentration was determined by measuring the absorbance at 280 nm using an extinction coefficient of 29 280 M^{-1} cm^{-1}.

In vitro assays of purified phosphotriesterases

The kinetic constants for the three substrates (MCO, MCS and dimethoate) were determined by varying the concentration of the substrate with a constant protein concentration. Hydrolysis of MCO and MCS was monitored by measuring the production of 3,5,6-trichloro-2-pyridinol spectrophotometrically at 310 nm ($\Delta\varepsilon_{310} = 5562$ M^{-1} cm^{-1}).[27,28] Hydrolysis of dimethoate was monitored by following the appearance of 2-nitro-5-thiobenzoate spectrophotometrically at 412 nm ($\Delta\varepsilon_{412} = 14\,145$ M^{-1} cm^{-1} at pH >7.5).[29] Assays of MCO and MCS were performed at 37 °C in 100 mM Tris.Cl pH 8.5, 10% methanol (to enhance the solubility of the substrates) and assays of dimethoate were performed at 25 °C in 100 mM Tris.Cl pH 8.5, 2% methanol, 1 mM DTNB. The k_{cat} and K_m values were determined by fitting the initial velocity data to the Michaelis–Menten equation. Assays were conducted in duplicate. Phosphotriesterases were diluted in 20 mM HEPES, 150 mM NaCl, pH 7.5 containing 0.1 mg ml^{-1} bovine serum albumin before use. In an attempt to measure the catalysis of TMP by OpdA, we incubated OpdA with various concentrations of TMP in 100 mM Tris.Cl pH 8.5, 10% methanol. An enzyme, GpdQ, known to hydrolyze dimethyl phosphate was then added to the reaction mixture to convert dimethyl phosphate to methyl phosphate, and calf intestinal alkaline phosphatase (Roche) was added to convert methyl phosphate to phosphate. Subsequently, the phosphate was assayed as described previously.[26]

Ab initio calculations

To assist in the interpretation of the experimental data, the relative energies of the reactants, products, transition structures and (where relevant) intermediates for the S_N2 substitution reactions were obtained *via* high-level *ab initio* calculations. These were performed on the model reaction shown in eqn. (2), and were carried out using GAUSSIAN 03.[30]

$$OH^- + Z{=}P(OCH_3)_2YR \rightarrow YR^- + Z{=}P(OCH_3)_2OH \qquad (2)$$

for relevant combinations of Z = O or S, Y = O or S, and R = CH_3, 3,5,6-trichloropyridin-2-yl, *p*-nitrophenyl or *S*-acetamide. The reactions with the 3,5,6-trichloropyridin-2-oxide (TCP), *p*-nitrophenoxide (NP), and *S*-acetamide leaving groups were treated as models of the reactions with the MCS, MCO, MPS, MPO and dimethoate pesticides, respectively. The geometries were optimized at the B3-LYP/6-31 + G(d) level of theory, and the zero-point energy was calculated using the scaled (by 0.9806) vibrational frequencies at this level.[31] Improved energies were then obtained at the MP2/6-311 + G(3df,2p) level of theory.

The accuracy of the RMP2/6-311 + G(3df,2p) level of theory was evaluated by comparing enthalpies obtained for the smaller $O{=}P(OCH_3)_3$ and $S{=}P(OCH_3)_3$ systems with calculations using a high level composite procedure, based on G3(MP2)-RAD. In this procedure, which we refer to as G3(MP2)-RAD(+), we replace the RCCSD(T)/6–31 G(d) and RMP2/6-31 G(d) calculations of the G3(MP2)-RAD method with calculations using the 6–31 + G(d) basis set so as to allow for a better description of the anionic species. The enthalpies (0 K, kJ mol^{-1}) of the reaction between $O/S{=}P(OCH_3)_3$ and OH^- to produce $CH3O^-$ and $O/S{=}P(OCH_3)_2OH$ were: −20.8 at G3(MP2)-RAD(+) and −15.9 at RMP2/6-311 + G(3df,2p) for O=P(OCH3)3; for $S{=}P(OCH_3)_3$ the corresponding values are −20.3 and −14.0, respectively. It is clear that there is a small systematic error when the RMP2/6-311 + G(3df,2p) level of theory is used, but this is well within normal acceptable levels. More importantly, the relative error between $O{=}P(OCH_3)_3$ and $S{=}P(OCH_3)_3$ is just 1.9 kJ mol^{-1}, and the MP2/6-311 + G(3df,2p) level of theory is thus sufficiently accurate for the present study.

Vibrational frequency and intrinsic reaction coordinate (IRC) calculations[32,33] were carried out to confirm transition states and local minima on the potential energy surface, and verify the connection of the transition states with local minima. To evaluate the suitability of the B3-LYP/6-31 + G(d) level of theory in optimizing transition states, we performed RMP2/6-311 + G(3df,2p) energy calculations on geometries provided by the IRC calculation of the transition state for MCO hydrolysis. Fig. 1 of the ESI† shows the relative energies at the B3-LYP/6-31 + G(d) and MP2/6-311 + G(3df,2p) levels of theory for the potential energy surface around the transition state. This demonstrates that while there is some difference in the location

of the transition state at the higher level of theory, the difference in the energy barrier is not significant (0.28 kJ mol^{-1}).

We evaluated the strength of the interaction between the coordinated Co^{2+} in the active site and MPS or OH^-. The structure of the β-Co^{2+} coordinated by simplified versions of the surrounding side chains ($N(CH_2)_2$ for His, CO_2 for Asp) was taken from the crystal structure,[7] and frozen. Formation of a complex with an optimized structure of MPS or OH^- was then examined. Owing to the size of the calculations, we used scans to find approximate geometries, rather than optimization. Consequently, the calculated values of the barriers are their upper bounds. This was accomplished using the LanL2DZ and B3-LYP/6-31 + G(d) basis sets.

pK_a and Log$P$ values

To evaluate the correlation between hydrophobicity and turnover rate the V_{max} data for a range of similar substrates (ethyl side chains, one-step hydrolysis in gas-phase), were taken from a previous study.[3] As a measure of hydrophobicity, the octanol–water partitioning coefficients, were taken from SciFinder Scholar, which was also used to acquire the pK_a values of the leaving groups.[34]

Conclusion

We have undertaken a detailed theoretical study into the hydrolysis of a range of phosphotriesters in the gas-phase in addition to experimental determination of the kinetic constants for the catalysis of their hydrolysis by OpdA. The aim of this was not to show that these calculations are a realistic model for the enzyme-catalyzed reaction; rather, by examining the differences between the theoretical data and experimental results, we have been able to highlight the steps in the mechanism where the enzyme lowers the activation energy and propose experimentally consistent explanations for the mechanism by which this occurs, citing previous kinetic and structural results. This demonstrates the utility of theoretical calculation in providing a more detailed understanding of the reaction that is being catalyzed by the enzyme. Other discrepancies between the enzyme-catalyzed results and the gas-phase hydrolysis, such as non-productive binding limiting the rate of substrate hydrolysis when the chemical step has no barrier, were able to be studied in significantly greater detail than would have been possible if the theoretical reactivity of the substrates were unknown. This examination of non-productive binding is significantly more detailed than other reported instances, and we expect that this effect may play a similarly important role in the enzymatic catalysis of highly reactive substrates in general.

Acknowledgements

We acknowledge generous allocations of computer time on the National Facility of the Australian Partnership for Advanced Computing and Australian National University Supercomputer Facility.

References

1 R. Kamanyire; and L. Karalliedde, *Occup. Med. (London)*, 2004, **54**, 69–75.
2 M. A. Sogorb, E. Vilanova and V. Carrera, *Toxicol. Lett.*, 2004, **151**, 219–233.
3 D. P. Dumas, S. R. Caldwell, J. R. Wild and F. M. Raushel, *J. Biol. Chem.*, 1989, **264**, 19659–19665.
4 I. Horne, T. D. Sutherland, R. L. Harcourt, R. J. Russell and J. G. Oakeshott, *Appl. Environ. Microbiol.*, 2002, **68**, 3371–3376.
5 H. Yang, P. D. Carr, S. Y. McLoughlin, J. W. Liu, I. Horne, X. Qiu, C. M. Jeffries, R. J. Russell, J. G. Oakeshott and D. L. Ollis, *Protein Eng.*, 2003, **16**, 135–145.
6 M. M. Benning, H. Shim, F. M. Raushel and H. M. Holden, *Biochemistry*, 2001, **40**, 2712–2722.
7 C. Jackson, H. K. Kim, P. D. Carr, J. W. Liu and D. L. Ollis, *Biochim. Biophys. Acta*, 2005, **1752**, 56–64.
8 S. D. Aubert, Y. Li and F. M. Raushel, *Biochemistry*, 2004, **43**, 5707–5715.
9 G. A. Omburo, J. M. Kuo, L. S. Mullins and F. M. Raushel, *J. Biol. Chem.*, 1992, **267**, 13278–13283.
10 C. M. Cho, A. Mulchandani and W. Chen, *Appl. Environ. Microbiol.*, 2004, **70**, 4681–4685.
11 N.-Y. Chang and C. Lim, *J. Am. Chem. Soc.*, 1998, **120**, 2156–2167.
12 N.-Y. Chang and C. Lim, *J. Phys. Chem. A*, 1997, **101**, 8706–8713.
13 J. Florian and A. Warshel, *J. Phys. Chem. B*, 1998, **102**, 719–734.
14 F. Zheng, C. Zhan and R. L. Ornstein, *J. Chem. Soc., Perkin Trans. 2*, 2001, **2**, 2355–2363.
15 V. E. Lewis, W. J. Donarski, J. R. Wild and F. M. Raushel, *Biochemistry*, 1988, **27**, 1591–1597.
16 S. B. Hong and F. M. Raushel, *Biochemistry*, 1996, **35**, 10904–10912.
17 K. Racke, D. Laskowski and M. Schlutz, *J. Agric. Food Chem.*, 1990, **38**, 1430–1436.
18 E. V. Patterson and C. J. Cramer, *J. Phys. Org. Chem.*, 1998, **11**, 232–240.
19 K. Lai, N. J. Stolowich and J. R. Wild, *Arch. Biochem. Biophys.*, 1995, **318**, 59–64.
20 D. W. Ingles and J. R. Knowles, *Biochem. J.*, 1967, **104**, 369–377.
21 A. Cornish-Bowden, *Fundamentals of Enzyme Kinetics*, Portland Press, London, 1995.
22 A. J. Oakley, J. Rossjohn, M. Lo Bello, A. M. Caccuri, G. Federici and M. W. Parker, *Biochemistry*, 1997, **36**, 576–585.
23 J. L. Vanhooke, M. M. Benning, F. M. Raushel and H. M. Holden, *Biochemistry*, 1996, **35**, 6020–6025.
24 D. M. Maxwell and K. M. Brecht, *Chem. Res. Toxicol.*, 1992, **5**, 66–71.
25 J. Koca, C. G. Zhan, R. C. Rittenhouse and R. L. Ornstein, *J. Am. Chem. Soc.*, 2001, **123**, 817–826.
26 S. Y. McLoughlin, C. Jackson, J. W. Liu and D. L. Ollis, *Appl. Environ. Microbiol.*, 2004, **70**, 404–412.
27 C. E. Furlong, R. J. Richter, S. L. Seidel, L. G. Costa and A. G. Motulsky, *Anal. Biochem.*, 1989, **180**, 242–247.
28 C. E. Furlong, R. J. Richter, S. L. Seidel and A. G. Motulsky, *Am. J. Hum. Genet.*, 1988, **43**, 230–238.
29 P. Eyer, F. Worek, D. Kiderlen, G. Sinko, A. Stuglin, V. Simeon-Rudolf and E. Reiner, *Anal. Biochem.*, 2003, **312**, 224–227.
30 M. J. Frisch, G. W. Trucks, H. B. Schlegel, G. E. Scuseria, M. A. Robb, J. R. Cheeseman, J. A. Montgomery Jr., T. Vreven, K. N. Kudin, J. C. Burant, J. M. Millam, S. S. Iyengar, J. Tomasi, V. Barone, B. Mennucci, M. Cossi, G. Scalmani, N. Rega, G. A. Petersson, H. Nakatsuji, M. Hada, M. Ehara, K. Toyota, R. Fukuda, J. Hasegawa, M. Ishida, T. Nakajima, Y. Honda, O. Kitao, H. Nakai, M. Klene, X. Li, J. E. Knox, H. P. Hratchian, J. B. Cross, C. Adamo, J. Jaramillo, R. Gomperts, R. E. Stratmann, O. Yazyev, A. J. Austin, R. Cammi, C. Pomelli, J. W. Ochterski, P. Y. Ayala, K. Morokuma, G. A. Voth, P. Salvador, J. J. Dannenberg, V. G. Zakrzewski, S. Dapprich, A. D. Daniels, M. C. Strain, O. Farkas, D. K. Malick, A. D. Rabuck, K. Raghavachari, J. B. Foresman, J. V. Ortiz, Q. Cui, A. G. Baboul, S. Clifford, J. Cioslowski, B. B. Stefanov, G. Liu, A. Liashenko, P. Piskorz, I. Komaromi, R. L. Martin, D. J. Fox, T. Keith, M. A. Al-Laham, C. Y. Peng, A. Nanayakkara, M. Challacombe, P. M. W. Gill, B. Johnson, W. Chen, M. W. Wong, C. Gonzalez, J. A. Pople, *Gaussian 03, Revision B.03*, Gaussian, Inc., Pittsburgh, PA, 2003.
31 A. P. Scott and L. Radom, *J. Phys. Chem.*, 1996, **100**, 16502–16513.
32 C. Gonzalez and H. B. Schlegel, *J. Chem. Phys.*, 1989, **90**, 2154–2161.
33 C. Gonzalez and H. B. Schlegel, *J. Phys. Chem.*, 1990, **94**, 5523–5527.
34 Calculated using Advanced Chemistry Development (ACD/Labs) Software Solaris V4.67, (1994-2005 ACD/Labs).